# Quaternary Ammonium-Containing Polyelectrolyte Brush Particles for Removal of Perrhenate Anion from Water: Effect of *N*-Substituents

*Kingsley O. Ojima, Sachini H. Dayarathne, Michael T. Kelly, and Bin Zhao*

Department of Chemistry, University of Tennessee, Knoxville, TN 37996, United States

Corresponding author: bzhao@utk.edu (B.Z.)

**Table of Content Graphic:**

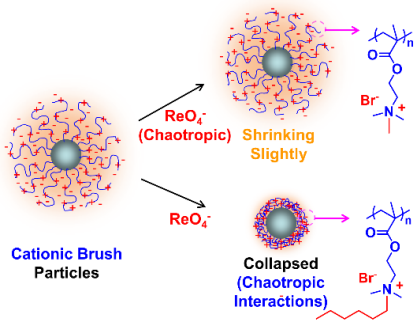


**Table of Content Text:** Quaternary ammonium-containing polyelectrolyte brush-grafted particles with various *N*-substituents are designed to remove perrhenate anion, a surrogate of radioactive pertechnetate, from water using the principle of chaotropic interactions. The brushes with longer alkyl or benzyl *N*-substituents underwent abrupt large size reduction transitions with addition of perrhenate and exhibited higher removal percentages of perrhenate in the absence and presence of competing anions.

**Abstract:** Radioactive pertechnetate ($TcO_4^-$) from the nuclear fuel cycle presents a severe risk to the environment due to its large solubility in water and non-complexing nature. By utilizing the chaotropic properties of $TcO_4^-$ and its nonradioactive surrogate perrhenate ($ReO_4^-$) and the

principle of chaotropic interactions, a series of quaternary ammonium-containing polyelectrolyte brush-grafted silica particles were designed and applied to remove $ReO_4^-$ from water. These cationic hairy particles (HPs) were synthesized by surface-initiated atom transfer radical polymerization of 2-(*N*,*N*-dimethylamino)ethyl methacrylate and subsequent quaternization with various halogen compounds. Dynamic light scattering (DLS) studies showed that the HPs with sufficiently long *N*-alkyl and *N*-benzyl substituents underwent sharp size reduction transitions in water when titrated with a $KReO_4$ solution, indicating strong chaotropic interactions between the brushes and $ReO_4^-$. All the HPs exhibited fast adsorption kinetics; the HPs with longer *N*-alkyl and *N*-benzyl substituents showed higher capabilities of removing $ReO_4^-$ than those with shorter *N*-alkyls. Moreover, the brush particles with longer *N*-substituents displayed a significantly stronger ability in selective adsorption of $ReO_4^-$ than the particles with shorter *N*-substituents in the presence of competing anions, such as $F^-$, $Cl^-$, $NO_3^-$, and $SO_4^{2-}$. This work opens a new avenue to design high-performance adsorbent materials for $TcO_4^-$ and $ReO_4^-$.

**Key Words:** Hairy Particles, Brush Particles, Cationic Polymer Brushes, Pertechnetate, Perrhenate, Chaotropic Effect, Quaternary Ammonium

## 1. Introduction

The management of technetium-99 ($^{99}Tc$), a persistent β-emitting fission product with a half-life of $2.13 \times 10^5$ years, is an important requirement in the advancement of nuclear energy.[1-3] This radioactive isotope is a byproduct of $^{235}U$ fission, with a yield of approximately 6%. It predominantly exists as the pertechnetate anion ($TcO_4^-$), a highly soluble and stable species with a solubility of 11.3 $molL^{-1}$ in water at 20 °C, in the nuclear fuel cycle and in the environment.[4,5] $TcO_4^-$ does not form strong complexes and exhibits a high environmental mobility, presenting a severe risk if poorly managed as it can infiltrate groundwater, accumulate in plants, and affect the food chain through aquatic ecosystems.[1-5] Exposure to $^{99}Tc$ through ingestion or prolonged contact can lead to serious health issues, including cancer, gastrointestinal disorders, and skin diseases.[6] The volatility of $TcO_4^-$ during the vitrification of nuclear waste and its interference in the extraction processes for uranium and plutonium recovery further complicate its remediation.[7]

The extraction and sequestration of $TcO_4^-$ from nuclear waste is critical for effective waste management and environmental protection.[1-3] Due to its anionic nature, cationic materials with fixed positive charges, such as anion-exchange resins,[8-10] cationic inorganic frameworks,[11,12] layered double hydroxides,[13-16] cationic metal-organic frameworks,[16-21] cationic polymeric networks,[1,4,7,22,23] have been evaluated for extracting $TcO_4^-$ or perrhenate ($ReO_4^-$) from water, and many of them have shown great promise. $ReO_4^-$ is a non-radioactive anion with a very similar molecular structure and almost identical physical and chemical properties in water to $TcO_4^-$ (e.g., ionic radii in water, 2.6 and 2.5 Å, respectively, and charge densities identical, 0.048 $e/Å^3$) and is often used as a surrogate for research in a laboratory setting.[1-3] Selective binding of $TcO_4^-$ and $ReO_4^-$ through supramolecular chemistry has also been explored as a means to remove them from

water.[3,24,25] Despite the tremendous progress made in recent years, many significant issues remain, such as efficiency and selectivity, which highlight the need for new advanced materials.[1-3]

$TcO_4^-$ and $ReO_4^-$ have a tetrahedral molecular geometry, a large size, and a low charge density.[1-3] When present in water, they disrupt the structure of water and decrease the number of hydrogen bonds in their solvation shell compared with bulk water, that is, they are water structure breakers, commonly called chaotropes.[26] This behavior is distinct from anions with a high charge density, such as $F^-$ and $SO_4^{2-}$, which enhance the hydrogen bonding of water (i.e., water structure makers or kosmotropes).[26-28] The difference can be seen from the small standard Gibbs energy of hydration for $TcO_4^-$ (-251 kJ/mol) compared with $F^-$ (-472 kJ/mol) and $SO_4^{2-}$ (-1090 kJ/mol).[1] The hydration energy of $ReO_4^-$ (-330 kJ/mol) is slightly higher than that of $TcO_4^-$,[2,3] suggesting that $TcO_4^-$ might be more chaotropic than $ReO_4^-$. In addition to having a tendency to form strong ion pairs with chaotropic cations in water, chaotropic anions, such as $ClO_4^-$ and $PF_6^-$, exhibit high affinities toward hydrophobic moieties, macrocyclic binding sites, and amphiphilic macromolecules in water as well as interfaces, an effect termed the chaotropic effect that has emerged as a driving force for supramolecular self-assembly.[29-31] For the hydrophobic effect-driven association of hydrophobic moieties in water,[32-34] ordered, ice-like water molecules around hydrophobic moieties are released into bulk water, resulting in a positive change for both entropy and enthalpy (i.e., favorable entropy change, $\Delta S > 0$, but an unfavorable enthalpy change, $\Delta H > 0$). In contrast, chaotropic interactions are driven by favorable enthalpic changes ($\Delta H < 0$) due to the release of less structured water molecules (i.e., less hydrogen bonded water molecules) from the chaotropic ions' solvation shells into bulk water to re-generate hydrogen bonds.[29,30]

We recently reported that three-arm star molecular bottlebrushes (SMBs) heterografted with poly(ethylene oxide) and either poly(2-(*N*,*N*-dimethylamino)ethyl methacrylate) (PDMAEMA) or

poly(2-(*N*,*N*-diethylamino)ethyl methacrylate) (PDEAEMA) side chains underwent shape transitions from star-like to globular in acidic water when sufficiently strong chaotropic anions, such as $ClO_4^-$ and $PF_6^-$, were added.[35] Very sharp size and shape transitions of SMBs were observed when superchaotropic anions, such as $[Fe(CN)_6]^{3-}$, were used. Intriguingly, the globular SMBs collapsed by moderately strong chaotropic anions, such as $ClO_4^-$ and $PF_6^-$, were found to be unfolded upon heating.[36] Excited by these results, we sought to use the principles of chaotropic interactions to design macromolecular brush materials for water treatment to remove toxic anions, such as $ClO_4^-$, $TcO_4^-$, and $ReO_4^-$, from aqueous solutions.

Macromolecular brush materials are featured by densely grafted brushes, where polymer chains are covalently tethered on a flat or curved solid surface (surface brushes)[37-40] or a polymer backbone (bottlebrushes).[41-43] Compared with other polymeric materials, including ion-exchange resins, surface brush materials exhibit a number of advantages as adsorbent materials.[44-47] Surface brushes are 3-dimensional with a unique, "open" brush structure,[37-40] allowing fast diffusion of ions into the brush layer and affording fast adsorption kinetics. The tunable chain lengths and high grafting densities afford a large number of functional groups, giving rise to high adsorption capacities. Polymer brushes are responsive materials that can assume stretched conformations or collapse in response to external stimuli.[39,40,48,49] When polymer brush-grafted particles (i.e., hairy particles, HPs, or brush particles) are employed, the particles can be readily dispersed in aqueous solutions, increasing the accessibility for adsorption processes. Surface polymer brushes are commonly synthesized by "grafting from",[37-40,50-58] where polymer chains are grown in situ from the initiator immobilized on the solid surface using a reversible deactivation radical polymerization method, such as atom transfer radical polymerization (ATRP) and reversible addition-

fragmentation chain transfer polymerization. The use of these "living"/controlled polymerization methods allows for precisely controlling the chain length and achieving narrow dispersities.[39,40]

In this work, we designed and synthesized a series of quaternary ammonium-containing polyelectrolyte brush-grafted silica particles with one *N*-substituent being systematically changed and applied these hairy particles to remove $ReO_4^-$ from water. The brush particles were synthesized by surface-initiated ATRP of 2-(*N*,*N*-dimethylamino)ethyl methacrylate and subsequent quaternization with various halogen compounds (Scheme 1). Six brush particle samples were synthesized from the same PDMAEMA brush-grafted particles and are denoted as Me-HPs (with one additional *N*-methyl substituent), Et-HPs (with one *N*-ethyl substituent), Pr-HPs (with one *N*-*n*-propyl), Bu-HPs (with one *N*-*n*-butyl), Hx-HPs (with one *N*-*n*-hexyl), and Bz-HPs (with one *N*-benzyl). We show that these brush particles are efficient adsorbents exhibiting fast adsorption kinetics and high removal percentages of $ReO_4^-$. Increasing the *N*-alkyl length or introducing an *N*-benzyl substituent enhances chaotropic interactions and the binding with $ReO_4^-$ and significantly improves the selectivity.

**Scheme 1. Synthesis of Quaternary Ammonium-Containing Polyelectrolyte Brush-Grafted Silica Particles by Surface-Initiated Atom Transfer Radical Polymerization and Post-polymerization Quaternization with Various Halogen Compounds**

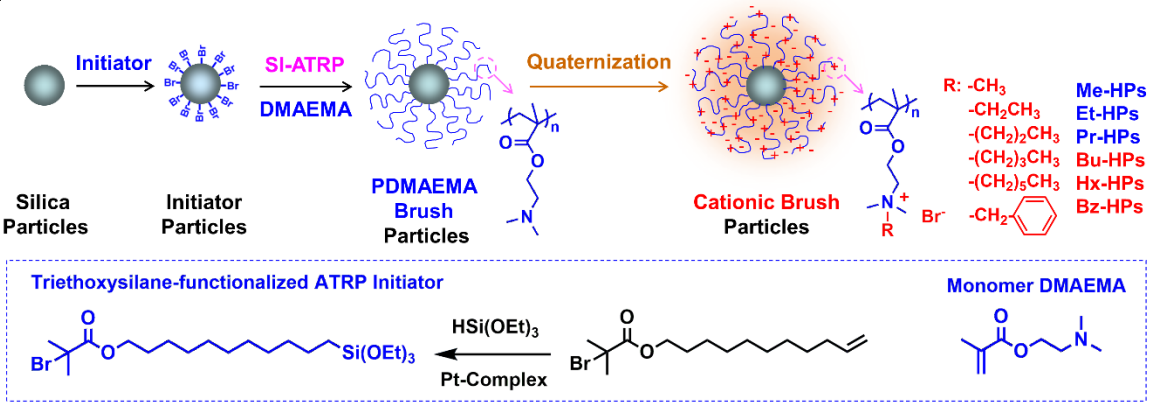

## 2. Experimental Section

Detailed experimental procedures are described in the Supporting Information.

## 3. Results and Discussion

### 3.1. Synthesis of PDMAEMA Brushes on Silica Particles by Surface-Initiated ATRP

PDMAEMA brush-grafted particles provide an excellent platform for preparing a series of distinct quaternary ammonium-containing polyelectrolyte brushes via quaternization with the only difference being one *N*-substituent, allowing for a systematic study of the effect of *N*-substituents on their interactions with $ReO_4^-$. We synthesized PDMAEMA brush-grafted silica particles by surface-initiated ATRP of 2-(*N*,*N*-dimethylamino)ethyl methacrylate from initiator-functionalized silica particles (Scheme 1). The initiator particles were made by the immobilization of a triethoxysilane-end-functionalized ATRP initiator, prepared by Pt-catalyzed hydrosilylation of 10-undecen-1-yl 2-bromo-2-methylpropionate with $HSi(OEt)_3$ (Scheme 1 bottom), on the surface of bare silica particles via a hydrolysis and condensation process.[59,60] The surface-initiated ATRP from the initiator particles was carried out at 75 °C in anisole in the presence of a free initiator, ethyl 2-bromoisobutyrate (EBiB), using CuCl/1,1,4,7,10,10-hexamethyltriethylenetetraamine as the catalyst. The addition of EBiB into the polymerization mixture not only produces a free polymer for convenient analysis of the polymer molecular weight and dispersity but also offers a better control of surface-initiated polymerization.[40] By using hydrofluoric acid to degraft the polymer brushes from silica particles, we and other researchers previously found that the molecular weights and the dispersities of the grafted polymers grown by surface-initiated reversible deactivation radical polymerization and the free polymers formed from the added free initiators were essentially identical.[40,51,52,59]

To achieve a high polymer content of PDMAEMA HPs and to exploit the unique structures and properties of polymer brushes as adsorbents, a large molar ratio of DMAEMA monomer to free initiator EBiB, 403, was used. The polymerization was monitored by $^1$H NMR spectroscopy and stopped when the monomer conversion reached 73.9%, determined by $^1$H NMR analysis of the final reaction mixture using the integrals of the peaks of -COOC$H_2$CH$_2$N- from the monomer at 4.28-4.24 ppm and the polymer at 4.14-4.02 ppm. From the monomer-to-free initiator EBiB molar ratio, the degree of polymerization (DP) of PDMAEMA was calculated to be 298. The PDMAEMA HPs were separated by centrifugation and purified by multiple cycles of dispersion in THF and centrifugation. From size exclusion chromatography (SEC) analysis, the free PDMAEMA polymer had an $M_{n,SEC}$ of 42.7 kDa and a $Đ$ of 1.15 (Figure S1), relative to linear polystyrene standards; the low $Đ$ indicates that the polymerization was well controlled. Thermogravimetric analysis (TGA) showed a large weight loss upon heating to ~ 800 °C compared with the initiator particles (Figure 1a), evidencing the successful growth of PDMAEMA brushes on the surface of silica particles. Figure 1b presents a representative transmission electron microscopy (TEM) micrograph of PDMAEMA HPs cast from a dispersion in acetonitrile onto a carbon-coated copper TEM grid. Analysis of 266 particles using Image-J software revealed an average diameter of 168.4 ± 17.3 nm for the core silica particles (additional TEM micrographs can be found in Figure S2 in the Supporting Information). Using the TGA data of the initiator particles and the PDMAEMA HPs, the $M_{n,cal}$ of PDMAEMA calculated from the DP, and the average diameter of core silica particles from TEM analysis, the grafting density (σ) of PDMAEMA brushes was calculated to be 0.64 chains/nm$^2$, similar to the values reported in the literature for the brushes grown on silica particles by surface-initiated ATRP.[60] (Detailed calculations of the σ can be found in the Supporting Information.) The average distance between grafting sites on the

surface of silica particles is 1.25 nm, which is about the projected length of 10 consecutive C-C bonds or 5 vinyl monomer units in the fully extended zig-zag conformation. Considering the DP = 298 of PDMAEMA, the grafted polymer chains are highly stretched and thus in the brush regime. The PDMAEMA brush-grafted silica particles were then used to prepare quaternary ammonium-containing polyelectrolyte brush particles by quaternization reactions with various halogen compounds.

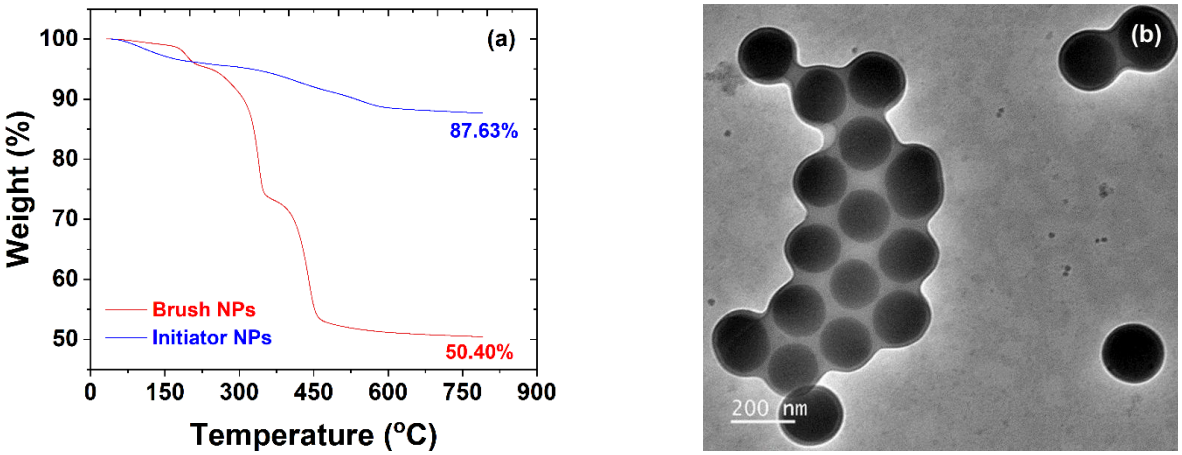


**Figure 1.** (a) Thermogravimetric analysis (TGA) of the initiator-functionalized silica particles and PDMAEMA hairy particles performed on a TA instruments Q-50 TGA under nitrogen at a heating rate of 20 °C/min from room temperature to 800 °C and (b) transmission electron microscopy micrograph of PDMAEMA brush particles drop cast from a dispersion in acetonitrile.

### 3.2. Synthesis of Quaternary Ammonium-Containing Polyelectrolyte Brush Particles from PDMAEMA HPs by Quaternization with Various Halogen Compounds

To systematically change the *N*-substituent for studying and utilizing the chaotropic interactions for removal of $ReO_4^-$, five *n*-alkyl halogen compounds (iodomethane, bromoethane, 1-bromopropane, 1-bromobutane, and 1-bromohexane) and benzyl bromide were used to quaternize the tertiary amine groups of PDMAEMA brushes (Scheme 1). To achieve a maximum degree of quaternization, ideally complete conversion, free PDMAEMA was first reacted with three equivalents of halogen compounds at 60 °C to test the reaction conditions. After 15 h, $^1H$

NMR analysis showed that the characteristic peak from -N($CH_3$)$_2$ of PDMAEMA at 2.20 – 2.50 ppm completely disappeared for all the halogen compounds except 1-bromohexane. Figure 2a shows the $^1$H NMR spectrum of the bromoethane-quaternized polymer; the $^1$H NMR spectra for other four fully quaternized polymers can be found in the Supporting Information (Figure S3). For the reaction with 1-bromohexane, a very small peak can still be seen at 2.43 ppm (Figure 2b) and remains visible even after an extended reaction time, for which the reason is unknown.

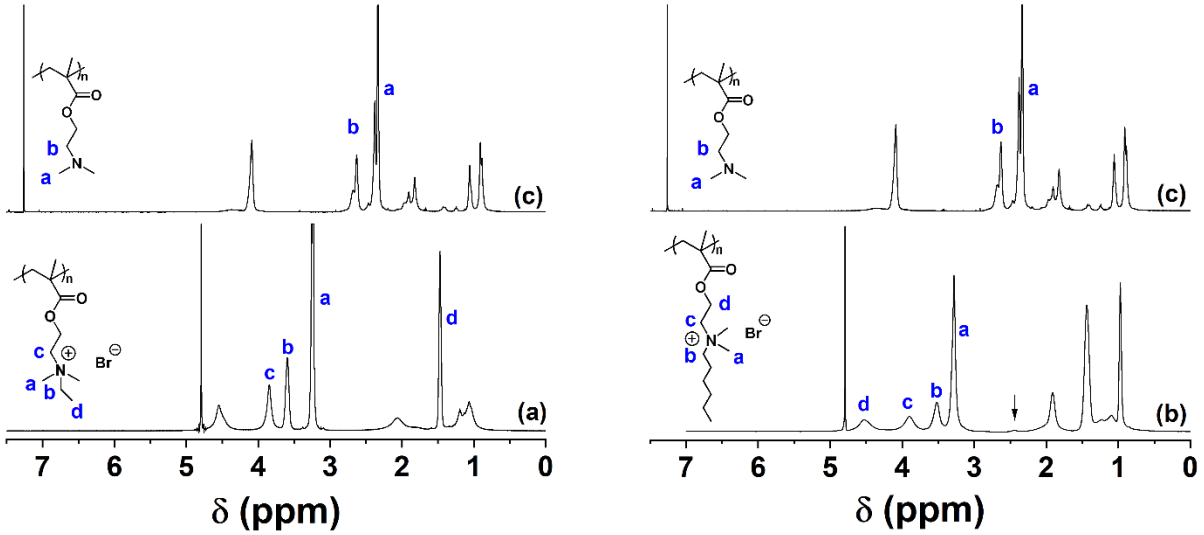


**Figure 2.** $^1$H NMR spectra of the ethyl-quaternized (a) and the *n*-hexyl-quaternized polymers (b) from the reactions of free PDMAEMA with bromoethane and 1-bromohexane, respectively, in $D_2O$. For comparison, the $^1$H NMR spectrum of the PDMAEMA in $CDCl_3$ is included (c).

Considering the densely grafted brush structure ($\sigma$ = 0.64 chains/nm$^2$), we increased the molar ratio of halogen compounds to the tertiary amine groups of PDMAEMA brushes to 6 : 1 and doubled the reaction time to 30 h for the quaternization reactions at 60 °C. After the reactions, the cationic HPs were isolated by centrifugation and washed via multiple cycles of re-dispersion (in acetonitrile and then water) and centrifugation. To better compare the adsorption capability for $ReO_4^-$, the iodide anion in the iodomethane-quaternized HPs were exchanged to bromide using a 4.0 M NaBr solution. The purified cationic HPs were freeze-dried and further dried under high

vacuum for TGA analysis (Figure S4). The quaternized brush particles are designated as Me-HPs (with one additional *N*-methyl substituent), Et-HPs (with an *N*-ethyl), Pr-HPs (with an *N*-*n*-propyl), Bu-HPs (with an *N*-*n*-butyl), Hx-HPs (with an *N*-*n*-hexyl), and Bz-HPs (with an *N*-benzyl). Using the TGA data of the quaternized HPs and initiator particles, the average diameter of silica particles, and the molecular weights of fully quaternized polymers (assumed), the grafting densities of the cationic polyelectrolyte HPs were calculated and are found to be similar (Table 1), suggesting that the quaternization reactions with six halogen compounds were complete or close to completion.

**Table 1.** Calculated Grafting Densities of Quaternary Ammonium-Containing Polyelectrolyte Brushes Grafted on Silica Particles

| Hairy Particles (HPs) [a] | Grafting Density (chains/nm$^2$) [b] |
|---|---|
| PDMAEMA HPs | 0.64 |
| Me-HPs | 0.65 |
| Et-HPs | 0.62 |
| Pr-HPs | 0.64 |
| Bu-HPs | 0.65 |
| Hx-HPs | 0.62 |
| Bz-HPs | 0.60 |

[a] PDMAEMA HPs: PDMAEMA brush-grafted silica particles. Degree of polymerization (DP) of PDMAEMA = 298; $M_{n,SEC}$ = 42.7 kDa and $Đ$ = 1.15 (relative to linear polystyrene standards). Me-HPs (methyl-quaternized HPs); Et-HPs (ethyl-quaternized HPs); Pr-HPs (*n*-propyl-quaternized HPs; Bu-HPs (*n*-butyl-quaternized HPs); Hx-HPs (*n*-hexyl-quaternized HPs); Bz-HPs (benzyl-quaternized HPs). [b] Grafting density was calculated using the TGA data of initiator particles and quaternized polymer brush particles, calculated molecular weight from DP = 298 assuming complete quaternization, and average diameter of core silica particles.

### 3.3. Dynamic Light Scattering (DLS) Studies of the Interactions of Quaternary Ammonium-Containing Brush Particles with Perrhenate Anion

As mentioned earlier, we previously observed that three-arm star bottlebrushes with poly(ethylene oxide) and PDMAEMA or PDEAEMA side chains in acidic aqueous solutions collapsed abruptly from a starlike to a globular shape with the addition of chaotropic anion-containing salts, such as $K_3[Fe(CN)_6]$ and $K_2S_2O_8$.[35,36] In contrast, only small decreases were

observed for NaBr and NaCl. The sharp size and shape transitions of these star brushes were attributed to chaotropic interactions. $ReO_4^-$ is a chaotropic anion, a water-structure breaker.[26] To study how different cationic HPs interact with $ReO_4^-$, DLS was employed. The brush particles were dispersed in Milli-Q water by ultrasonication at a concentration of 0.10 mg/g, and a 10.0 mM aqueous solution of $KReO_4$ was added under stirring condition in aliquots of 5.0 μL using a microsyringe. After equilibration for a sufficient amount of time, Z-average hydrodynamic diameters ($D_h$) of brush particles were measured. The results are summarized in Figure 3a in plots of $D_h$ versus the injected total volume of the 10.0 mM solution of $KReO_4$ for all six quaternary ammonium-containing brush particle samples.

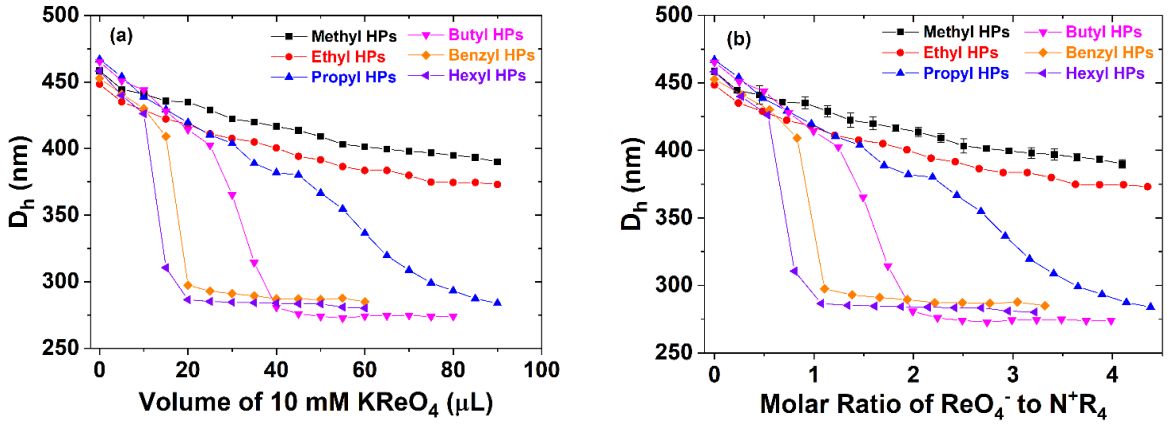


**Figure 3.** Plots of Z-average hydrodynamic diameter ($D_h$), measured by DLS, of 0.1 mg/g hairy particles in Milli-Q water at 25 °C vs added volume of a 10 mM $KReO_4$ solution (a) or calculated molar ratio of added $ReO_4^-$ to ammonium cations (b) for Me- (square), Et- (circle), Pr- (up-pointing triangle, Bu- (down-pointing triangle), Bz- (diamond), and Hx-HPs (left-pointing triangle).

In the absence of $KReO_4$, the $D_h$ values of all six brush particle samples in water at a concentration of 0.1 mg/mL were similar, ~ 460 nm. TEM analysis of Et-HPs cast from a 0.1 mg/g aqueous dispersion showed that the positively charged ammonium-containing polyelectrolyte brush particles appeared to be fully, individually dispersed in Milli-Q water (Figure S5). With the gradual addition of a 10.0 mM $KReO_4$ solution, the particle samples exhibited distinctly different

behaviors, depending on their *N*-substituents. Me-HPs showed small and steady decreases in size and ended at 390 nm when 90.0 μL of the aqueous $KReO_4$ solution was added. A similar behavior was observed for Et-HPs; however, the size of this particle sample was consistently lower by ~ 15 nm than that of Me-HPs throughout the titration and ended at 373 nm. In stark contrast, sharp size reduction transitions were observed for Bz-, Hx-, and Bu-HPs, particularly, Bz- and Hx-HPs. For example, the $D_h$ of Hx-HPs was 426.2 nm at 10.0 μL of the $KReO_4$ solution; after the injection of just another aliquot of 5.0 μL, the $D_h$ decreased sharply to 310.5 nm and eventually leveled off to 280 nm after more $KReO_4$ was added. For Bu-HPs, the transition was slower and occurred over a period of three aliquots (15 μL) of the $KReO_4$ solution, but the size decrease, ~ 122 nm from 25 to 40 μL of $KReO_4$, was comparable to that for Hx- and Bz-HPs. Interestingly, Pr-HPs exhibited an intermediate behavior; initially, small and smooth $D_h$ decreases, similar to those of Me- and Et-HPs, were observed till about 45 μL of the $KReO_4$ solution, followed by larger size reductions in the range of 45 μL to 80 μL, which resembled the size reduction transitions of Hx-, Bz-, and Bu-HPs. The eventual $D_h$ value was similar to those of Hx- and Bz-HPs.

To gain a better understanding about the size reduction transitions of cationic HPs, we calculated the molar ratios of added $KReO_4$ to the ammonium groups in each sample (1.00 g) at a concentration of 0.1 mg/g and re-plotted $D_h$ as a function of $[KReO_4]/[NR_4^+]$ (Figure 3b). It is interesting to note that the sharp size reduction transition for Bz-HPs occurred at the molar ratio of $ReO_4^-$ to ammonium cation ($NR_4^+$) of ~ 1 : 1. The molar ratio is slightly smaller for Hx-HPs, ~ 0.7 : 1. For Bu- and Pr-HPs, the middle points (molar ratios) of the transitions are at ~ 1.6 : 1 and 3.2 : 1, respectively. Thus, DLS studies showed that with increasing the *N*-*n*-alkyl length from methyl to hexyl in cationic HPs, the interactions between the cationic brushes and $ReO_4^-$ are stronger, as evidenced by the larger size decreases from Me- to Et- and Pr-HPs and the sharp size

reduction transitions at small molar ratios of $ReO_4^-$ to $NR_4^+$ from Bu- to Hx-HPs. Bz-HPs exhibited a similar behavior to Hx-HPs.

Given the same +1 charge on the nitrogen atom for all six cationic hairy particle samples, the observations cannot be explained by simple electrostatic attractive interactions. According to Marcus, $(CH_3)_4N^+$ is a chaotropic cation, while $(C_2H_5)_4N^+$ is a borderline ion between chaotropic and kosmotropic cations.[26] On the other hand, *n*-$C_4H_9N^+$ is a kosmotropic cation,[26] likely because the four *n*-butyl groups invoking the hydrophobic effect. Thus, by comparison, the methyl-quaternized ammonium cation is most likely a chaotrope, while the ammonium cation containing an *N*-ethyl group is either a chaotropic or a borderline anion. For *n*-butyl, *n*-hexyl, and benzyl groups, water form more ordered ice-like structures around them; this increased hydrophobic effect may make their quaternized ammonium cations behave as kosmotropic cations, despite the presence of two small *N*-methyl groups. Thus, the chaotropic effect is most likely the main cause for the large and sharp size reduction transitions exhibited by Hx- and Bz-HPs in the titration of $KReO_4$, though ion pairing may also make some contributions. Since the collapse of the brushes occurred at a $ReO_4^-$-to-$NR_4^+$ molar ratio of ~ 0.7 : 1 for Hx-HPs, earlier than that for Bz-HPs, Hx-HPs likely exhibited stronger chaotropic interactions with $ReO_4^-$, which presumably arises from its long linear alkyl structure. Stronger interactions between cationic groups in the brush particles and perrhenate would result in stronger adsorption of $ReO_4^-$ from water.

For comparison, titration experiments were also performed using KF, KCl, $KNO_3$, or $K_2SO_4$ by DLS for Et- and Hx-HPs in water, two representative samples that showed distinct behaviors in response to $KReO_4$ (Figure 3). Note that $F^-$ and $SO_4^{2-}$ are kosmotropic anions that increase the number of surrounding hydrogen bonds by 0.12 and 0.78,[29] respectively. $Cl^-$ is a borderline anion,[26-29] while $NO_3^-$ is a chaotrope.[26] Initially, a 10 mM KCl solution was used to titrate a 0.10

mg/g dispersion of Hx-HPs (1.00 g), and the $D_h$ of the particles was found to decrease slightly, by 13.6 nm, after 100.0 µL of the 10 mM KCl solution was added (Figure S6). The featureless and small changes indicate weak interactions between the brushes and $Cl^-$ as expected. We then increased the concentration to 100 mM for all four salts for the titration of two particle samples, and the DLS results are shown in Figure 4. Note that at the end of titration, 100 µL of a 0.10 M salt solution was added for each salt, that is, 0.58 mg of KF, 0.75 mg of KCl, 1.10 mg of $KNO_3$, and 1.74 mg of $K_2SO_4$ were added into the 0.10 mg/g particle dispersions (1.00 g initial mass).

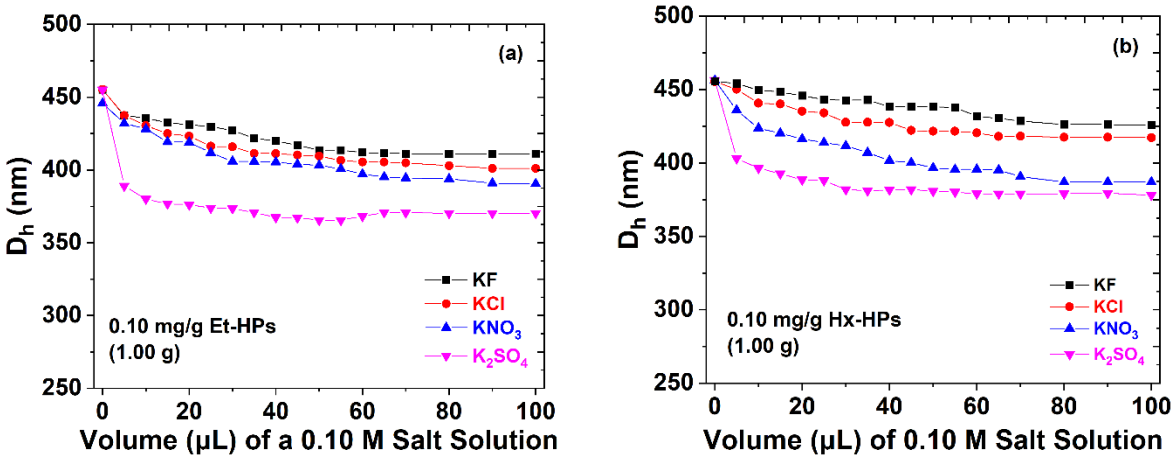


**Figure 4.** Plot of $D_h$, measured by DLS, of 0.10 mg/g Et- (a) and Hx-HPs (b) in Milli-Q water at 25 °C vs added volume of a 0.10 M aqueous solution of KF (square), KCl (circle), $KNO_3$ (up-pointing triangle), and $K_2SO_4$ (down-pointing triangle).

For both Et- and Hx-HPs, the size decreases were small and steady with the gradual addition of KF and KCl; the overall size changes were 44 nm and 54 nm for Et-HPs, and 31 and 38 nm for Hx-HPs, respectively. The slightly smaller decreases for Hx-HPs suggest a slightly weaker interaction of the brushes in this sample with $F^-$ and $Cl^-$, which is understandable as $F^-$ is a kosmotrope and $Cl^-$ is a borderline anion.[26,27] For $KNO_3$, the size decrease for Hx-HPs was noticeably larger than that of Et-HPs (69.2 nm vs 55 nm), but there was no sharp size transition,

indicating that the interaction of Hx-HPs with $NO_3^-$ is stronger than $F^-$ and $Cl^-$ but weaker than $ReO_4^-$. This can be attributed to the chaotropic effect because nitrate is a chaotrope exhibiting a higher affinity toward the *N*-*n*-hexyl groups in Hx-HPs. Thus, Figures 3 and 4 showed that the chaotropicity increased in the order of $F^- < Cl^- < NO_3^- << ReO_4^-$ and that stronger interactions were observed between Hx-HPs and $NO_3^-$ and $ReO_4^-$ presumably due to the chaotropic effect.[29] In contrast to KF, KCl, $KNO_3$, a large decrease was observed for both Et- and Hx-HPs with the injection of only 5.0 μL of 0.100 M $K_2SO_4$ (~ 60 nm), and after that the change became slower. The relatively large size reductions after the injection of the first 5 μL aliquot are very likely caused by the divalent nature of sulfate anion that allows it to interact with two ammonium cations simultaneously (i.e., a "crosslinking" effect). The similar size decreases for both particle samples suggest that the divalent nature of $SO_4^{2-}$ is likely the predominant factor. Nevertheless, these size changes are much smaller than that in the collapse of the brushes in Hx-HPs by $ReO_4^-$ (140 nm, Figure 3). The small and smooth decreases after the first 5 μL are similar to those for $F^-$, thus consistent with the kosmotropic nature (i.e., the high charge density) of sulfate anion.

### 3.4. Kinetics of Adsorption of $ReO_4^-$ by Cationic HPs

Kinetics studies of adsorption of $ReO_4^-$ by six cationic HP samples were conducted first to determine the times needed to reach saturation. For each particle sample, seven aqueous solutions of 30 mM $KReO_4$ and 0.2 mg/g HPs were prepared and stirred at room temperature for various amounts of time, ranging from 10 to 150 min. The particles were then isolated by centrifugation, and the supernatant liquid was promptly transferred to a polypropylene conical tube for inductively coupled plasma optical emission spectroscopy (ICP-OES) analysis to measure the concentration of $ReO_4^-$. Figure 5 shows the removal percentage of $ReO_4^-$ as a function of time. For all six brush particle samples, the removal percentages were high and the adsorption essentially reached

saturation before 20 min. This observation indicated that the adsorption of $ReO_4^-$ by the HPs was fast, which can be attributed to the unique "open" brush structure allowing fast diffusion of $ReO_4^-$ into the interior of the brushes. Note that the removal percentage of $ReO_4^-$ at 150 min was 92.5 ± 2.0% for Me-HPs, 94.2 ± 0.2% for Et-HPs, 95.3 ± 0.2% for Pr-HPs, 97.9 ± 1.8% for Bu-HPs, 98.1 ± 2.3% for Bz-HPs, and 98.4 ± 2.0% for Hx-HPs, which is in the same order of the interaction strength of these cationic HPs with $ReO_4^-$ observed from the DLS studies. All these brush particles performed better than the imidazolium-containing covalent polymer network-1 (CPN-1, removal percentage of $ReO_4^-$ = 90.0%) and CPN-2 (91.0%) but lower than CPN-3 (> 99.9%) recently reported by Wang et al. under similar conditions (0.2 mg/mL sorbent and [$ReO_4^-$] = 28 ppm).[61] In particular, the adsorption capabilities of Hx- and Bz-HPs for $ReO_4^-$ anion are only slightly lower than CPN-3. It should be noted here that in our adsorption experiments the polymer concentration is < 0.2 mg/mL because of the silica core in the brush particles (see the TGA data of six hairy particle samples in Figure S4). Our results demonstrate the great potential of macromolecular brush materials in the removal of toxic oxyanions from water for water treatment.

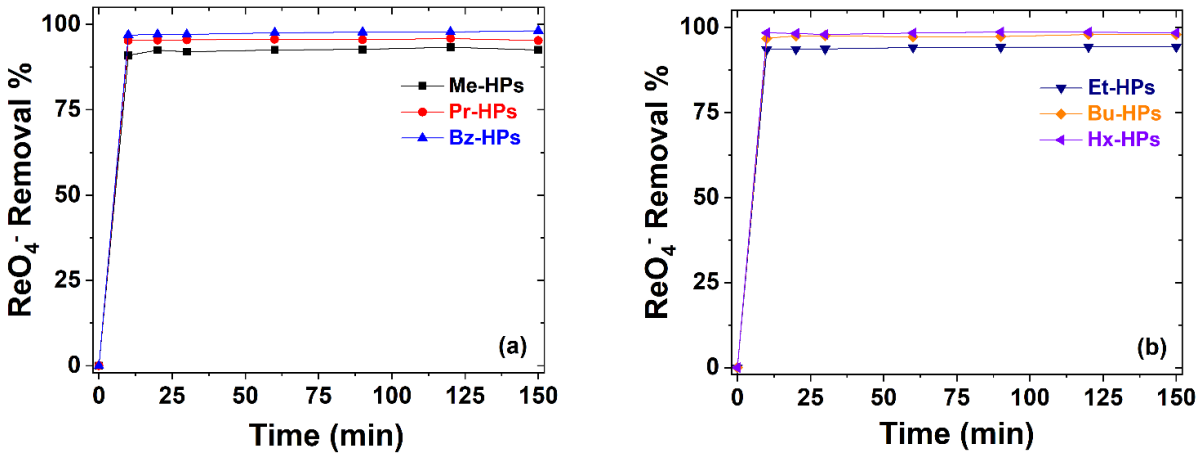


**Figure 5.** Plot of removal percentage of $ReO_4^-$ versus adsorption time using 30 mM $KReO_4$ and 0.2 mg/g cationic HPs (a: Me-, Pr-, and Bz-HPs; b: Et-, Bu-, and Hx-HPs).

### 3.5. Adsorption of $ReO_4^-$ by Cationic HPs: Effects of Brush *N*-Substituent and Particle Concentration

We then studied the effect of particle concentration on the removal of $ReO_4^-$ from water by varying the particle concentration while keeping the $KReO_4$ concentration constant. Five different particle concentrations, 1.0, 0.50, 0.20, 0.10, and 0.050 mg/g, were used in this experiment for all HPs with a total of 10.00 g for the mixtures at the same concentration of $KReO_4$ (30 ppm). Since the kinetics studies showed that the adsorption of $ReO_4^-$ by cationic HPs reached saturation in < 20 min, we stirred the mixtures for 2 h to ensure that maximum adsorption was reached and then separated the HPs by centrifugation. The concentrations of $ReO_4^-$ in the supernatant liquids were measured, and the results are summarized in Figure 6.

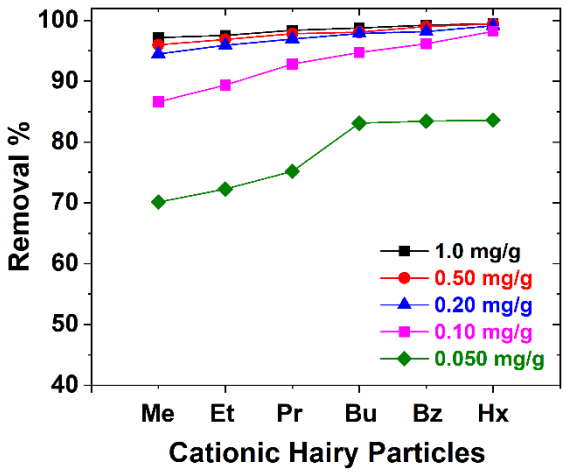


**Figure 6.** Effect of particle concentration on the removal percentage of $ReO_4^-$ from water for Me-, Et-, Pr-, Bu-, Hx-, and Bz-HPs. The concentration of $KReO_4$ was kept at 30.0 ppm for all these adsorption experiments. (For clarity, only removal percentages of $ReO_4^-$ are shown here; the plots including standard deviations can be found in the Supporting Information, Figure S7.)

Figure 6 shows that for all five concentrations, there is a clear trend that the removal percentage of $ReO_4^-$ increased in the order from Me- to Et-, Pr-, Bu-, Bz-, and Hx-HPs. For particle concentrations of 1.0, 0.50, and 0.20 mg/g, the differences between Me- and Hx HPs are small, 2.3% at the concentration of 1 mg/g and 4.6% at 0.2 mg/g. The difference became larger with

decreasing the concentration of HPs to 0.10 and 0.050 mg/g, about 12-14% from Me- to Hx-HPs. Note that the removal percentages for the six particles at a concentration of 0.2 mg/g in Figure 6 essentially overlapped with the data from kinetics study (Figure S8), highlighting the reproducibility of the adsorption experiments. Combining the observations for the particle concentrations of 0.10 mg/g and 0.050 mg/g, Hx-, Bz-, and Bu-HPs showed higher capabilities of removing $ReO_4^-$ than Me- and Et-HPs, while Pr-HPs exhibited an intermediate ability between the two groups. This is in line with the observations from DLS titration experiments, where sharp size reduction transitions were observed for Hx-, Bz-, and Bu-HPs, whereas Me- and Et-HPs exhibited small and gradual decreases in $D_h$. Pr-HPs displayed a behavior in between Et- and Bu-HPs, with the first part of the curve resembling Et-HPs and the second part showing a transition at a molar ratio of 3.2, broader than that of Bu-HPs. Thus, with changing the alkyl group from methyl to *n*-hexyl and introducing benzyl as an *N*-substituent in quaternary ammonium cation, HPs showed an increasing ability to adsorb $ReO_4^-$, which can be attributed to the stronger interactions of the ammonium cation with $ReO_4^-$ that presumably arose from the higher affinity of $ReO_4^-$ toward the hydrophobic moieties of the brushes in water.

We note here that the average distance between the grafting sites for the six particle samples from the grafting densities in Table 1 was in the range of 1.24 – 1.29 nm, which is about the projected length of five vinyl monomer units in the zig-zag conformation. When moving away from the surface of silica particles, there is more space for the grafted polymer chains due to the curvature. The ionic radius of $ReO_4^-$ in water is 2.6 Å,[2,3] and thus, the diffusion of $ReO_4^-$ into the brush layer should not be limited by the brush grafting density for these charged brush particles. However, if the grafting density is very high, e.g., ≥ 1.2 chains/nm$^2$ as we reported before,[62] the diffusion of $ReO_4^-$ could be affected, and its adsorption may be adversely impacted. On the other

hand, if the grafting density is low, the amount of the grafted polymer chains (or the amount of quaternary ammonium groups) per unit mass of hairy particles would be low, which would lead to a lower adsorption capacity for perrhenate. Presumably, there is an optimal grafting density for brush particles to exhibit the best performance for removal of $ReO_4^-$ anion.

### 3.6. Adsorption of $ReO_4^-$ by Et- and Hx-HPs in the Presence of Other Anions

We further studied the adsorption of $ReO_4^-$ in the presence of other anions with various concentrations by Et- and Hx-HPs, the two representative particle samples from the two groups based on the DLS studies and $ReO_4^-$ adsorption experiments. Four salts, KF, KCl, $KNO_3$ and $K_2SO_4$, which were used for the titration of Et- and Hx-HPs in water (Figure 4), were selected for studies of competitive adsorption with $ReO_4^-$. The mass concentration ratio of $KReO_4$ to each of the four salts was varied from 1 : 1 to 1 : 10, and then 1 : 100, while the concentrations of $KReO_4$ and HPs were kept at 30.0 ppm and 0.20 mg/g, respectively. Thus, the concentration of the second salt was 0.030, 0.30, and 3.0 mg/g for the three mass ratios. Figure 7 shows the results from these studies, and several general trends can be seen. (i) For all four salts, with increasing concentration of the second salt from 0.030 to 0.30 and 3.0 mg/g, the adsorption of $ReO_4^-$ decreased but to a different degree for the two particle samples. The decreases for Hx-HPs are much smaller than those for Et-HPs. At a mass ratio of 1 : 1, the adsorption of $ReO_4^-$ by Hx-HPs was barely affected by the presence of competing anions, whereas the decreases were more noticeable for Et-HPs except KF. In contrast, large differences were seen at a mass ratio of 1 : 100; the removal percentages of $ReO_4^-$ by Et-HPs were 78.87% (KF), 33.15% (KCl), 13.83% ($KNO_3$), and 46.99% ($K_2SO_4$), whereas for Hx-HPs they were 91.94% (KF), 68.75% (KCl), 35.82% ($KNO_3$), and 72.43% ($K_2SO_4$), which are significantly higher than those for Et-HPs (2-3 times in the cases of KCl and $KNO_3$). These data revealed that Hx-HPs exhibited a better selectivity for $ReO_4^-$ in the presence

of other anion than Et-HPs, which is attributed to the stronger interactions between $ReO_4^-$ and the brushes that likely arise from the chaotropic effect as seen from DLS studies (Figures 3 and 4). (ii) Among the four salts, KF shows the smallest effect in decreasing the removal percentage of $ReO_4^-$ at all three mass ratios. This is understandable because $F^-$ is a kosmotrope and thus has little interference in the chaotropic interactions of chaotropic $ReO_4^-$ with the brushes.

(iii) The extent of decrease in the removal of $ReO_4^-$ followed the same order, KF < KCl < $KNO_3$, at all three mass ratios. This agrees with the observations from DLS studies (Figure 4) and the order of the chaotropicity for the three anions reported in the literature ($F^-$ < $Cl^-$ < $NO_3^-$). Anions with a higher chaotropicity cause a larger interference in the adsorption of $ReO_4^-$ by the brushes. Note that in the DLS study of the titration of Et- and Hx-HPs in water by $KNO_3$, we observed a larger decrease in $D_h$ for Hx-HPs than Et-HPs (69.2 nm vs 55 nm for a total of 1.10 mg $KNO_3$ added to 1.00 g solution). The adsorption of $ReO_4^-$ in Figure 7 at a mass ratio of 1 : 100 (3.0 mg $KNO_3$ per g) was 35.82% for Hx-HPs, almost three times that by Et-HPs under the same conditions (13.83%). This can be explained by the much stronger interactions of Hx-HPs with $ReO_4^-$ than with $NO_3^-$. (vi) Sulfate anion exhibited a behavior that is not in line with other three anions (Figure 7). At the mass ratio of 1 : 1, $SO_4^{2-}$ decreased the removal percentage of $ReO_4^-$ by the largest amount for both particle samples, which is likely due to its divalent nature that results in intra- or intermolecular "crosslinking" as seen in the DLS studies in Figure 4. At the mass ratio of 1 : 10, sulfate caused the second largest decrease in the removal percentage of $ReO_4^-$. Further increasing the mass ratio to 1 : 100, the effect of $SO_4^{2-}$ was only larger than $F^-$. Thus, at higher mass ratios, it appears that the kosmotropic property of sulfate becomes more important than its divalent nature. Again, the decreases in the removal of $ReO_4^-$ by Hx-HPs caused by sulfate are significantly smaller than Et-HPs at all three mass ratios, demonstrating its better anti-interference

property than Et-HPs. In summary, Hx-HPs exhibited a significantly better capability of removing $ReO_4^-$ than Et-HPs in the presence of both kosmotropic and chaotropic competitive anions.

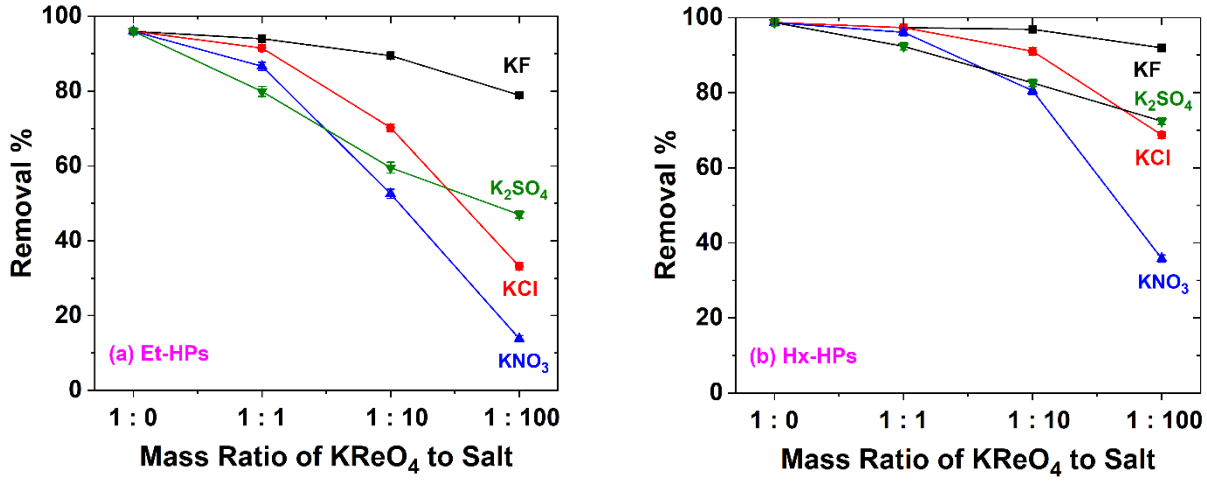


**Figure 7.** Removal percentage of $ReO_4^-$ in the presence of KF, $K_2SO_4$, KCl, and $KNO_3$ with a mass concentration ratio of 1 : 1, 1 : 10, and 1 : 100 for $KReO_4$ to the second salt for (a) Et-HPs and (b) Hx-HPs. For all these adsorption experiments, the concentrations of $KReO_4$ and hairy particles were kept to be the same, 30.0 ppm and 0.20 mg/g, respectively.

### 3.7. DLS Studies of Et and Hx-HPs with Gradual Addition of $KReO_4$ in the Presence of Another Salt

Figure 7 shows that the presence of other anions negatively affected the removal of $ReO_4^-$ by HPs, especially Et-HPs. To better understand how those anions affects the interactions of $ReO_4^-$ with the brush, we conducted DLS measurements by titrating 0.10 mg/g Et- and Hx-HPs dispersed in Milli-Q with a 10 mM $KReO_4$ solution in the presence of KF, KCl, $KNO_3$, or $K_2SO_4$. The concentrations of these salts were varied from 1.04 mM to 10.0 mM, and 0.100 M in order to probe their effects on the interactions of cationic brushes with $ReO_4^-$. Figures 8 and 9 show the plots of $D_h$ vs volume of 10 mM $KReO_4$ in the presence of the four salts at the three concentrations for Hx- and Et-HPs, respectively. Remarkably, the pronounced size reduction transition of Hx-HPs was seen at all three concentrations of KF (Figure 8a), though it shifted to a higher volume of $KReO_4$ and became broader with increasing the concentration of KF from 1.04 mM (0.060 mg/g KF) to

10.0 mM (0.58 mg/g) and 0.100 M (5.8 mg/g). This indicates that $F^-$ exerts little influence on the interactions of the brushes with $ReO_4^-$, which can be attributed to the vast different solution properties of the two anions in water as discussed earlier. This observation correlates well with the results from adsorption experiments (Figure 7); the removal of $ReO_4^-$ with an initial concentration of 30 ppm by Hx-NPs decreased only slightly from 98.7% to 96.86% in the presence of 0.30 mg/g KF (mass ratio of 1 : 10) and 91.94% in the presence of 3.0 mg/g KF (mass ratio of 1 : 100).

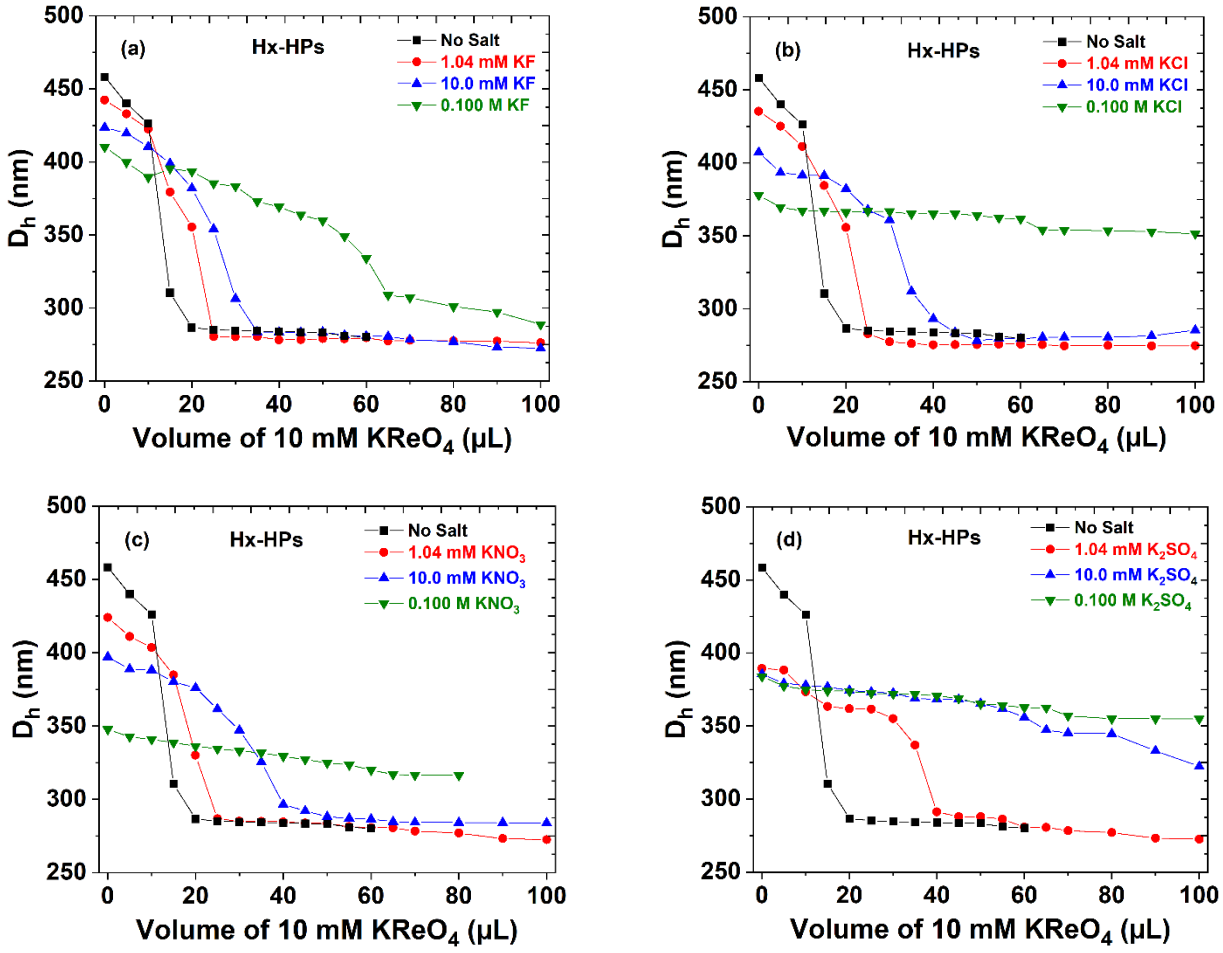


**Figure 8.** Plots of $D_h$ of 0.10 mg/g Hx-HPs in Milli-Q water in the presence of 1.04 mM, 10.0 mM, and 0.100 M KF (a), KCl (b), $KNO_3$ (c), or $Na_2SO_4$ (d) from DLS measurements with gradual addition of a 10 mM $KReO_4$ solution in aliquots of 5 μL.

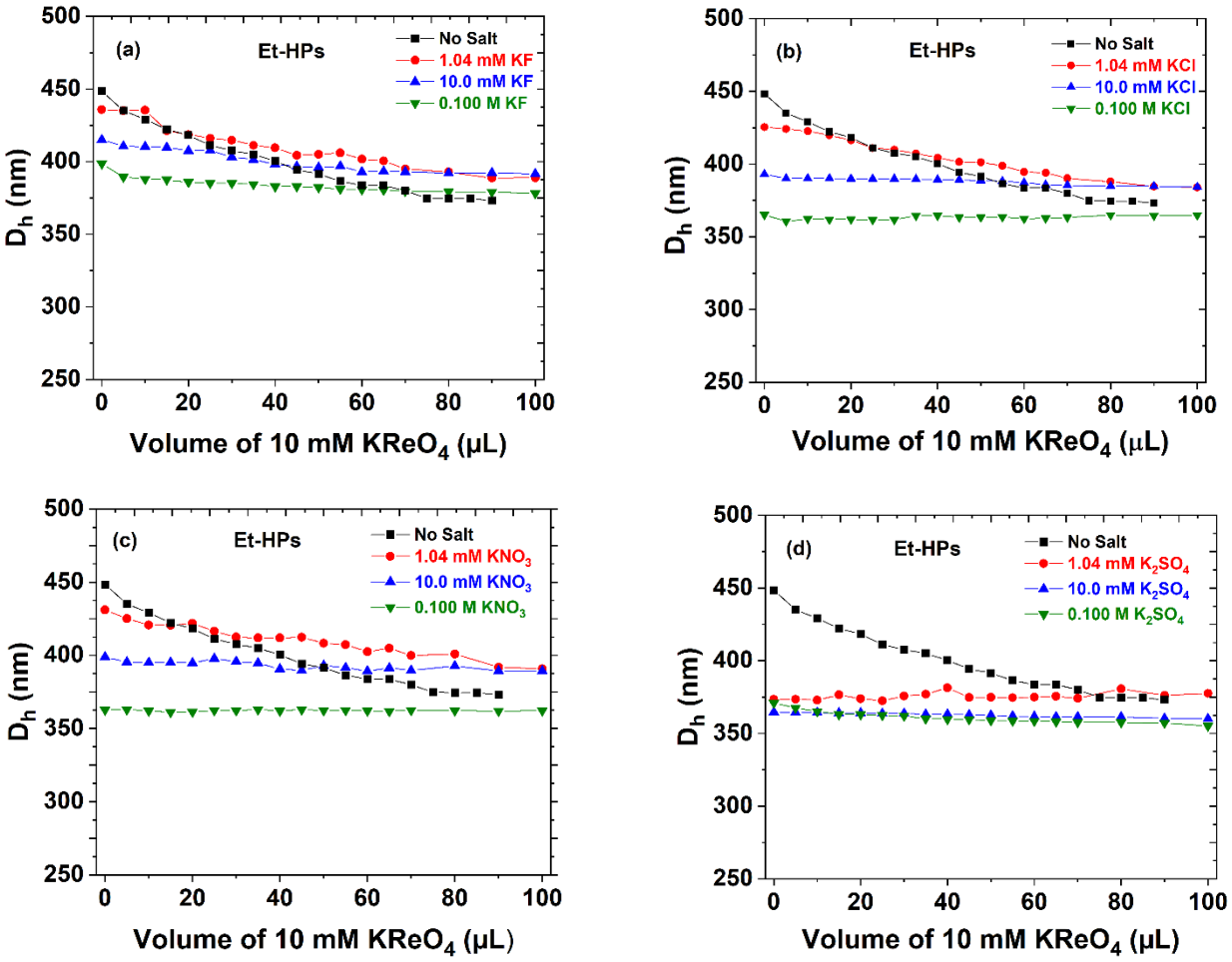


**Figure 9.** Plots of $D_h$ of 0.10 mg/g Et-HPs in Milli-Q water in the presence of 1.04 mM, 10.0 mM, and 0.100 M KF (a), KCl (b), $KNO_3$ (c), or $Na_2SO_4$ (d) from DLS measurements with gradual addition of a 10 mM $KReO_4$ solution in aliquots of 5 μL.

For KCl and $KNO_3$, the size transitions of Hx-HPs were observed at concentrations of 1.04 mM (0.078 mg/g for KCl and 0.12 mg/g for $KNO_3$) and 10.0 mM (0.75 mg/g for KCl and 1.1 mg/g for $KNO_3$) (Figure 8b,c). However, further increasing the concentration to 0.100 M (7.5 mg/g for KCl and 11.1 mg/g for $KNO_3$), only a smaller steplike decrease is visible at ~ 60 μL for KCl and $KNO_3$, indicating that at such a high concentration of the second salt, the preferential adsorption of $ReO_4^-$ is largely lost. These observations agree with the adsorption data in Figure 7, where the removal percentages of $ReO_4^-$ remained high at a mass ratio of 1 : 10, 91.02% for KCl and 80.52%

for $KNO_3$ (0.30 mg/g salt, in between 1.04 and 10.0 mM in the titration experiments in Figure 8, and thus the size transition is expected to be visible). Increasing the mass ratio to 1 : 100 (3.0 mg/g, in between 10.0 and 100.0 mM in Figure 8, and thus the size transition either diminished significantly or disappeared), there was a large decrease in the adsorption of $ReO_4^-$ (Figure 7b, $ReO_4^-$ removal percentage: 68.75% for KCl and 35.82% for $KNO_3$). For $K_2SO_4$, at a concentration of 1.04 mM, the transition is still sharp but smaller in magnitude and shifted to a larger volume of the $KReO_4$ solution (Figure 8d). The transition at the concentration of 10.0 mM became much broader, and only the initial portion was visible. When 100 mM $K_2SO_4$ was present, only a small decrease could be seen. This is likely caused by the divalent nature of sulfate anion, and the resultant "crosslinking" complicated the response of Hx-HPs to the gradual addition of $KReO_4$ and apparently diminished the size reduction transition. Nevertheless, there were only moderate losses in the removal of $ReO_4^-$ (82.61% and 72.43% at mass ratios of 1 : 10 and 1 : 100, respectively).

For Et-HPs, when the concentration of the second salt was 1.04 mM, the titration curves were similar to those in Milli-Q water for KF, KCl, and $KNO_3$ (Figure 9a,b,c), suggesting that the interactions of Et-HPs with $ReO_4^-$ were not significantly affected. This correlates well with the results from the adsorption experiments in the presence of these salts that the removal percentages of $ReO_4^-$ were high (94.0%, 91.47%, and 86.61% in the presence of 30 ppm KF, KCl, and $KNO_3$, respectively) (Figure 7). Increasing the concentrations to 10.0 and 100.0 mM, while the $D_h$ of Et-HPs still showed decreases with gradual addition of $KReO_4$ in the presence of KF (Figure 9a, overall size decrease: 23.4 and 20.6 nm for 10.0 and 100.0 mM KF, respectively), the curves for KCl and $KNO_3$ were nearly unchanged (Figure 9b,c, 8.8 nm and 9.5 nm decrease at 10 mM, respectively, and essentially no change, < 1 nm, at 100.0 mM). These observations suggest that Et-HPs still showed preferential adsorption of $ReO_4^-$ in the presence of 10.0 and 100.0 mM KF,

but the selectivity was largely lost for KCl and $KNO_3$ at the same concentrations as can be see from the data in Figure 7. For $K_2SO_4$, the titration curves at all three concentrations were essentially unchanged (Figure 9d), suggesting a strong interference of sulfate in the interactions of Et-HPs with $ReO_4^-$, in contrast to the titration curves of Hx-HPs, where even at a concentration of 100.0 mM, one can still see the gradual decrease in $D_h$. This could explain the stronger effect of $K_2SO_4$ in decreasing the removal percentages of $ReO_4^-$ by Et-HPs compared with Hx-HPs in Figure 7.

From Figures 3, 4, and 7-9, we can draw two conclusions. (i) For KF, KCl, and $KNO_3$ as well as $KReO_4$, the size changes of cationic HPs in the titration curves are consistent with the order of increasing chaotropicity $F^- < Cl^- < NO_3^- << ReO_4^-$. The higher the chaotropicity of an anion, the higher the ability of the anion in competing for the brushes, as reflected in the order of decreasing removal percentage of $ReO_4^-$. (ii) For Hx-HPs, the characteristic sharp size reduction transition with gradual addition of $KReO_4$ was preserved at all three concentrations for KF, at concentrations of 1.04 and 10.0 mM for KCl and $KNO_3$, and at 1.04 mM for $K_2SO_4$, while the size changes of Et-HPs at the same concentrations of the salts were significantly smaller or essentially zero. This suggests that Hx-HPs exhibit a higher selectivity toward $ReO_4^-$ than Et-HPs under the same conditions, which correlates well with the results from adsorption experiments in the presence of a second salt.

## 4. Conclusions

Six quaternary ammonium-containing cationic brush particle samples were synthesized by quaternization of PDMAEMA brushes grafted silica particles with iodomethane, 1-bromoethane, 1-bromopropane, 1-bromobutane, 1-bromohexane, and benzyl bromide and used as adsorbents for removal of $ReO_4^-$ from water. DLS studies of these brush particles in Milli-Q water with gradual addition of $KReO_4$ revealed that Hx-, Bz-, and Bu-HPs underwent sharp size reduction transitions,

which are attributed to the chaotropic effect, whereas only small, gradual decreases in $D_h$ were seen for Me- and Et-HPs. All of the brush particles exhibited fast kinetics in the adsorption of $ReO_4^-$, which is believed to be a result of the unique, "open" brush structure. Hx-, Bz-, and Bu-HPs exhibited a higher ability in removing $ReO_4^-$ than Me- and Et-HPs under the same conditions, especially at lower particle concentrations. When other anions, such as $F^-$, $Cl^-$, $NO_3^-$, and $SO_4^{2-}$, were present, Hx-HPs displayed a significantly stronger ability in selective adsorption of $ReO_4^-$ than Et-HPs, agreeing well with the results from DLS studies of HPs with addition of 10 mM $KReO_4$ in the presence of KF, KCl, $KNO_3$, and $K_2SO_4$ with various concentrations. This work represents the first example of using HPs along with the principle of chaotropic interactions to design brush materials to remove $ReO_4^-$ from water. As mentioned in the Introduction, $TcO_4^-$ is likely more chaotropic than $ReO_4^-$ and thus could exhibit even stronger chaotropic interactions with, e.g., Hx-HPs, making its separation even more efficient than $ReO_4^-$ in the absence or presence of competing anions. Given the vast tunability of brush structure, the diversity of polyelectrolytes, and the number of possible elements as the central atom of cations, exciting opportunities can be envisioned to design high-performance adsorbent materials to remove from water toxic chaotropic anions, not only $TcO_4^-$ and $ReO_4^-$ but also possibly other oxyanions such as $ClO_4^-$,[63] by utilizing the unique structure and responsiveness of polymer brushes and the principle of chaotropic interactions.

**ORCID:** Bin Zhao: 0000-0001-5505-9390

**Supporting Information.** The Supporting Information is available from the Wiley Online Library or from the author.

**Acknowledgements:** B.Z. thanks NSF for the support (DMR-2004564 and -2412257). The authors thank Professor Ziling (Ben) Xue for helpful discussion.

**Conflict of Interest**
The authors declare no conflict of interest.

**Data Availability Statement**

The data that support the findings of this study are available in the Supporting Information.

**References**


1. C. Xiao, A. Khayambashi, S. Wang, *Chem. Mater*. **2019**, *31*, 3863.
2. D. Banerjee, D. Kim, M. J. Schweiger, A. A. Kruger, P. K. Thallapally, *Chem. Soc. Rev*. **2016**, *45*, 2724.
3. E. A. Katayev, G. V. Kolesnikov, J. L. Sessler, *Chem. Soc. Rev*. **2009**, *38*, 1572.
4. L. Zhu, C. Xiao, X. Dai, J. Li, D. Gui, D. Sheng, L. Chen, R. Zhou, Z. Chai, T. E. Albrecht-Schmitt, S. Wang, *Environ. Sci. Technol. Lett*. **2017**, *4*, 316.
5. J. P. Icenhower, N. P. Qafoku, J. M. Zachara, W. J. Martin, *Am. J. Sci*. **2010**, *310*, 721.
6. Y. Gao, K. Chen, X. Tan, X. Wang, A. Alsaedi, T. Hayat, C. Chen, *ACS Sustain. Chem. Eng*. **2017**, *5*, 2163.
7. J. Li, X. Dai, L. Zhu, C. Xu, D. Zhang, M. A. Silver, P. Li, L. Chen, Y. Li, D. Zuo, H. Zhang, C. Xiao, J. Chen, J. Diwu, O. K. Farha, T. E. Albrecht-Schmitt, Z. Chai, S. Wang, *Nat. Commun*. **2018**, *9*, 3007.
8. B. Gu, G. M. Brown, P. V. Bonnesen, L. Liang, B. A. Moyer, R. Ober, S. D. Alexandratos, *Environ. Sci. Technol*. **2000**, *34*, 1075.
9. P. V. Bonnesen, G. M. Brown, S. D. Alexandratos, L. B. Bavoux, D. J. Presley, V. Patel, R. Ober, B. A. Moyer, *Environ. Sci. Technol*. **2000**, *34*, 3761.
10. J. Li, L. Zhu, C. Xiao, L. Chen, Z. Chai, S. Wang, *Radiochim. Acta,* **2018**, *106*, 581.
11. S. Wang, P. Yu, B. A. Purse, M. J. Orta, J. Diwu, W. H. Casey, B. L. Phillips, E. V. Alekseev, W. Depmeier, D. T. Hobbs, T. E. Albrecht-Schmitt, *Adv. Funct. Mater*. **2012**, *22*, 2241.
12. S. Zhong, X. Li, Y. Wang, D. Han, J. Peng, Y. Hao, L. Zhao, J. Li, M. Zhai, *ACS Sustain. Chem. Eng.* **2021**, *9*, 7379.
13. M. J. Kang, S. W. Rhee, H. Moon, V. Neck, T. Fanghanel, *Radiochim. Acta* **1996**, *75*, 169.
14. M. J. Kang, K. S. Chun, S. W. Rhee, Y. Do, *Radiochim. Acta* **1999**, *85*, 57.
15. Y. Wang, H. Gao, J. *Colloid Interface Sci*. **2006**, *301*, 19.
16. G. Sheng, Y. Tang, W. Linghu, L. Wang, J. Li, H. Li, X. Wang, Y. Huang, *Appl. Catal. B* **2016**, *192*, 268.
17. J. Li, X. Wang, G. Zhao, C. Chen, Z. Chai, A. Alsaedi, T. Hayat, X. Wang, *Chem. Soc. Rev.* **2018**, *47*, 2322.
18. P. Kumar, A. Pournara, K.-H. Kim, V. Bansal, S. Rapti, M. J. Manos, *Prog. Mater. Sci.* **2017**, *86*, 25.
19. D. Sheng, L. Zhu, C. Xu, C. Xiao, Y. Wang, Y. Wang, L. Chen, J. Diwu, J. Chen, Z. Chai, T. E. Albrecht-Schmitt, S. Wang, *Environ. Sci. Technol.* **2017**, *51*, 3471.
20. D. Sheng, L. Zhu, L. X. Dai, C. Xu, P. Li, C. I. Pearce, C. Xiao, J. Chen, R. Zhou, T. Duan, O. K. Farha, Z. Chai, S. Wang, *Angew. Chem. Int. Ed.* **2019**, *58*, 4968.
21. C.-P. Li, H.-R. Li, J.-Y. Ai, J. Chen, M. Du, *ACS Cent. Sci.* **2020**, *6*, 2354.
22. J. S. Lee, H. M. Luo, G. A. Baker, S. Dai, *Chem. Mater.* **2009**, *21*, 4756.
23. J. Li, B. Li, N. Shen, L. Chen, L. Guo, L. Chen, L. He, X. Dai, Z. Chai, S. Wang, *ACS Cent. Sci.* **2021**, *7*, 1441.
24. R. Alberto, G. Bergamaschi, H. Braband, T. Fox, V. Amendola, *Angew. Chem. Int. Ed.* **2012**, *51*, 9772.
25. D. Zhang, T. K. Ronson, J. Mosquera, A. Martinez, J. R. Nitschke, *Angew. Chem. Int. Ed.* **2018**, *57*, 3717.

26. Y. Marcus, *Chem. Rev.* **2009**, *109*, 1346.
27. K. D. Collins, *Biophys. J.* **1997**, *72*, 65.
28. K. Collins, *Methods* **2004**, *34*, 300.
29. K. I. Assaf, W. M. Nau, *Angew. Chem. Int. Ed.* **2018**, *57*, 13968.
30. K. I. Assaf, W. M. Nau, *Org. Biomol. Chem.* **2023**, *21*, 6636.
31. Y. Li, Y. Wang, G. Huang, X. Ma, K. Zhou, J. Gao, *Angew. Chem. Int. Ed.* **2014**, *53*, 8074.
32. N. T. Southall, K. A. Dill, A. D. J. Haymet, *J. Phys. Chem. B* **2002**, *106*, 521.
33. D. Chandler, *Nature* **2005**, *437*, 640.
34. N. Wang, B. T Seymour, E. M. Lewoczko, E. W. Kent, M.-L. Chen, J.-H. Wang, B. Zhao. *Polym. Chem.* **2018**, *9,* 5257.
35. E. W. Kent, E. M. Lewoczko, B. Zhao, *Polym. Chem.* **2021**, *12*, 265.
36. E. M. Lewoczko, M. T. Kelly, E. W. Kent, B. Zhao, *Soft Matter* **2021**, *17*, 6566.
37. B. Zhao, W. J. Brittain, *Prog. Polym. Sci.* **2000**, 25, 677.
38. Y. Tsujii, K. Ohno, S. Yamamoto, A. Goto, T. Fukuda, *Adv. Polym. Sci.* **2006**, *197*, 1.
39. B. Zhao, L. Zhu, *Macromolecules* **2009**, *42*, 9369.
40. A. J. Chancellor, B. T. Seymour, B. Zhao, *Anal. Chem.* **2019**, *91*, 6391.
41. S. S. Sheiko, B. S. Sumerlin, K. Matyjaszewski, *Prog. Polym. Sci.* **2008**, *33*, 759.
42. B. Zhao, *J. Phys. Chem. B* **2021**, *125*, 6373.
43. M. T. Kelly, Z. Chen, T. P. Russell, B. Zhao, *Angew. Chem. Int. Ed.* **2023**, *62*, e202315424.
44. A. Farrukh, A. Akram, A. Ghaffar, S. Hanif, A. Hamid, H. Duran, B. Yameen, *ACS Appl. Mater. Interfaces* **2013**, *5*, 3784.
45. X. Wang, S. Jing, Y. Liu, X. Qiu, Y. Tan, *RSC Adv.* **2017**, *7*, 13112.
46. A. Dolatkhah, L. D. Wilson, *ACS Appl. Mater. Interfaces* **2016**, *8*, 5595.
47. F. Chi, S. Zhang, J. Wen, J. Xiong, S. Hu, *J. Mater. Sci.* **2019**, *54*, 3572.
48. J. M. Horton, Z. Bai, X. Jiang, D. Li, T. P. Lodge, B. Zhao, *Langmuir* **2011**, *27*, 2019.
49. Y. Eygeris, Q. Wang, M. Görke, M. Grünwald, I. Zharov, *ACS Appl. Mater. Interfaces* **2023**, *15*, 29384.
50. J. Pyun, K. Matyjaszewski, *Chem. Mater.* **2001**, *13*, 3436.
51. M. Husseman, E. E. Malmstrom, M. McNamara, M. Mate, D. Mecerreyes, D. G. Benoit, J. L. Hedrick, P. Mansky, E. Huang, T. P. Russell, C. J. Hawker, *Macromolecules* **1999**, 32, 1424.
52. D. J. Li, X. Sheng, B. Zhao, *J. Am. Chem. Soc.* **2005**, 127, 6248.
53. K. Ohno, T. Morinaga, S. Takeno, Y. Tsujii, T. Fukuda, *Macromolecules* **2007**, 40, 9143.
54. J. M. Horton, S. D. Tang, C. H. Bao, P. Tang, F. Qiu, L. Zhu, B. Zhao, *ACS Macro Lett.* **2012**, *1*, 1061.
55. R. A. E. Wright, K. Wang, J. Qu, B. Zhao, *Angew. Chem. Int. Ed.* **2016**, *55*, 8656.
56. J. Yan, T. Kristufek, M. Schmitt, Z. Wang, G. Xie, A. Dang, C. M. Hui, J. Pietrasik, M. R. Bockstaller, K. Matyjaszewski, *Macromolecules* **2015**, *48*, 8208.
57. C. A. Bohannon, A. J. Chancellor, M. T. Kelly, T. T. Le, L. Zhu, C. Y. Li, B. Zhao, *J. Am. Chem. Soc.* **2021**, *143*, 16919.
58. R. Yin, P. Chmielarz, I. Zaborniak, Y. Zhao, G. Szczepaniak, Z. Wang, T. Liu, Y. Wang, M. Sun, H. Wu, J. Tarnsangpradit, M. R. Bockstaller, K. Matyjaszewski, *Macromolecules* **2022**, *55*, 6332.
59. K. Ohno, T. Morinaga, K. Koh, Y. Tsujii, T. Fukuda, *Macromolecules* **2005**, 38, 2137.
60. C. H. Bao, S. D. Tang, J. M. Horton, X. M. Jiang, P. Tang, F. Qiu, L. Zhu, B. Zhao, *Macromolecules* **2012**, 45, 8027.

61. B. Wang, J. Li, H. Huang, B. Liang, Y. Zhang, L. Chen, K. Tan, Z. Chai, S. Wang, J. T. Wright, R. W. Meulenberg, S. Ma, *ACS Cent. Sci.* **2024**, *10*, 426.
62. X. Jiang, B. Zhao, G. Zhong, N. Jin, J. M. Horton, L. Zhu, R. S. Hafner, T. P. Lodge. *Macromolecules* **2010**, 43, 8209-8217.
63. D. P. Chen, C. Yu, C.-Y. Chang, Y. Wan, J. M. J. Frechet, W. A. Goddard III, M. S. Diallo, *Environ. Sci. Technol.* **2012**, 46, 10718.